JOURNAL OF MODERN OPTICS, 2000, VOL. 47, NO. 7, 1237–1246

A variable lateral-shearing Sagnac interferometer with high numerical aperture for measuring the complex spatial coherence function of light

CHUNG-CHIEH CHENG, M. G. RAYMER

Oregon Center for Optics and Department of Physics, University of Oregon, Eugene, OR 97403, USA

and H. HEIER

Division for Electronics, Norwegian Defence Research Establishment, N-2007 Kjeller, Norway

(*Received 13 July 1999; accepted 25 October 1999*)

Abstract. We combine a telescopic imaging system with a common-path, lateral-shearing interferometer and use phase-shifting interferometry to measure the complex spatial coherence function (or mutual intensity) of a linearly-polarized optical field. Our telescopic design increases the numerical aperture of the system without distorting the shape of the wave front, and therefore without changing the phase difference between lateral positions in the optical field. Our method of generating lateral-sheared images introduces no additional astigmatism. To demonstrate the use of the interferometer we extract the information contained in the complex spatial coherence function to reconstruct the amplitude and phase of a coherent optical field, and we also show how the spatial coherence function evolves from a coherent field to a partially coherent one as light traverses a random multiple-scattering medium.

1. Introduction

All light fields existing in nature are, strictly speaking, partially coherent. The so-called coherent and incoherent fields are special cases with proper limits on the coherence length scale. The spatial coherence function (SCF) (also called mutual intensity or two-point field correlation function), of a one-dimensional optical field $E(x)$ may be defined as [1]

$$\Gamma(x+s/2,x-s/2) \equiv \langle E(x+s/2)E^{*}(x-s/2)\rangle, \tag{1}$$

where x is a spatial position, s is a shear, and the $\langle\,\rangle$ indicates an ensemble average over the possible forms of the scalar electric field $E(x)$, each being associated with a particular configuration of the environment subject to spatial or temporal fluctuations.

A better understanding of partially coherent light is not only fundamentally interesting but also essential in many research areas. Measurement of the SCF plays an important part in characterizing the statistical properties of partially coherent light. For example, it can determine the dielectric correlation function of an inhomogeneous random medium (for example, biotissue [2]), can reveal the

large-scale stellar cluster distribution in the galaxy [3], and can provide information on the generalized radiance used in radiative transfer [4]. Methods have been developed for imaging internal structure of transparent scattering objects through measurement of the SCF of partially coherent light scattered from the object [5]. The SCF also carries information about the properties of sources of light. For example, a laser beam can be usefully characterized by its degree of spatial coherence.

In spite of the importance of the SCF there is a surprising lack of convenient methods for quantitative measurement of this function (for a discussion of early methods see Francon and Mallick [6]). A recent method developed by Iaconis and Walmsley [7] (referred to below as IW) utilized a variable-lateral-shearing, common-path (Sagnac) interferometer to measure the SCF. In this method the beam amplitude is split into two copies which counter-propagate around a ring and, before recombining, are sheared transversely relative to one another by passing through a variably tilted, thick glass block with parallel sides. The sheared and recombined beams interfere and the resulting intensity pattern is recorded with a charge-coupled device (CCD) camera. Unfortunately the shearing block introduces astigmatism into the beam and can lead to errors in the measurement. Furthermore, since it uses no lense before the interferometer, this design has a rather small collection numerical aperture (NA), typically around 0.01, limited by the length of the interferometer and the diameters of the optical elements used in its construction. This limits the amount of light that can be collected, and also the achievable spatial resolution, which is set by diffraction. If one tries to increase the NA by simply placing a collection lens between source and interferometer, then the phase structure of the optical fields acquires a large extra quadratic component (corresponding to a spherical wave front) which is inconvenient for data processing. For these reasons the IW design is best suited for analysing collimated or weakly divergent beams. However, there are cases in which one would like to measure the SCF of highly divergent light, for example, the light transmitted through a random, multiple-scattering medium, such as a biological tissue [2, 8, 9]. This motivated our effort to generalize the design of IW.

In this paper we report an improved interferometric imaging system that can measure a complex SCF with greater light collection efficiency than in the previous design by IW and with no introduced astigmatism. The main innovations are the use of a telescopic imaging system, a free-space shearing method and a four-phase, phase-shifting method for acquiring the data. After describing the operation of the imaging interferometer, we illustrate its operation in the cases of a coherent laser beam and a laser beam which has travelled through a random, multiple-scattering medium.

2. Principles of lateral-shearing stationary PSI

To measure a complex SCF we use lateral shearing and phase-shifting interferometry (PSI) [10]. The basic concept is to split the input beam into two identical copies, spatially separated by a distance (shear) s, and record the interferogram of these two beams:

$$I^{(\delta)}(x,s) = \langle |E(x+s/2) + E(x-s/2)|^2 \rangle$$
$$= \langle |E(x+s/2)|^2 \rangle + \langle |E(x-s/2)|^2 \rangle$$
$$+ \mathrm{Re}\,[2\langle E(x+s/2)E^*(x-s/2)\rangle \exp(\mathrm{i}\delta)], \quad (2)$$

where δ is the phase shift between these two sheared beams and $\mathrm{Re}[\cdots]$ stands for the real part of the quantity inside the square brackets. The removal of the first two terms in the right-hand side of equation (2) can be achieved by using stationary PSI, which is based on processing the interferograms for several different values of δ. We have designed an apparatus that can be adjusted to select $\delta = 0$ or π to make the sign of the last term of equation (2) opposite, and by subtracting these two interference patterns we obtain the real part of the SCF. Similarly we can select $\delta = \frac{1}{2}\pi$ or $\frac{3}{2}\pi$ and subtract the resulting interferograms to obtain the imaginary part of the SCF. Combining these two parts yields the complex SCF. This procedure involves same-pixel subtractions without using complicated mathematical procedures to retrieve information as in previous experiments employing phase-space tomography [11].

3. Optical system and measurement

Figure 1 shows our set-up. It is similar in layout to that of IW, with several key differences, as mentioned above. Light from the sample or source (S) leaves the aperture (AP) having 1 mm diameter, is collected by lenses L1, L2, then is linearly polarized by a polarizing cube (P), and passes through a nominal

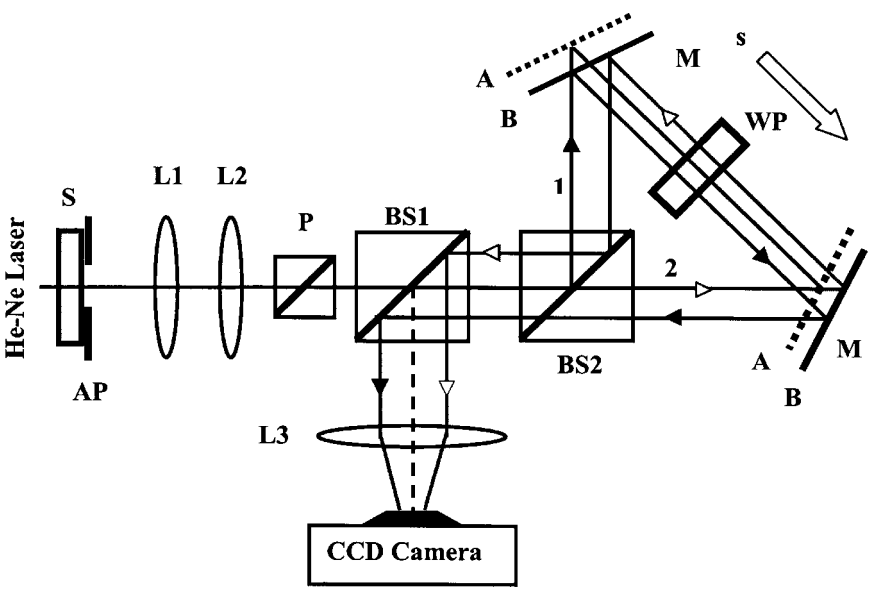

Figure 1. The surface of the source (S), primary or secondary, is imaged using three lenses onto a CCD camera. The light enters the interferometer (BS1 and BS2 are non-polarizing 50/50 beam splitters), which measures the spatial coherence function (SCF) of the transmitted light. M, mirror; P, linear polarizer; L1, L2, L3, lenses; AP, aperture; WP, wave plate set.

50/50 non-polarizing beam splitter (BS1) before entering the Sagnac interferometer through the second beam splitter (BS2). The light is equally split into clockwise- and counterclockwise-travelling beams, which undergo shears of equal magnitude, but opposite sign, before recombining at BS2, where interference takes place. After reflecting partially from BS1 the light is imaged onto the CCD camera where its interferogram is recorded.

There are different ways to shear light laterally [12]. In our design the shears are introduced by moving a pair of mirrors (M) parallel to the propagation axis of the middle portion of the triangular ring. Figure 1 illustrates moving the mirrors from a position 'A' to position 'B' by a common translation stage and the subsequent optical paths followed by a single ray in the two cases. This free-space shearing avoids the introduction of astigmatism, which will occur if instead one uses a tilted glass block to create shears. In our system, which is designed to have a relatively large numerical aperture, avoidance of astigmatism is important.

A key concern of our design is to increase the NA of the system. To achieve this, we need to consider three different aspects of the design. The first is to ensure that the Lagrange invariant (or throughput; etendue) of the system is determined by the size of the components that are most difficult to enlarge; the other concerns minimizing the instrument contribution to the phase difference between different parts of the object. Finally, we need a sharp image of the object.

It turns out that for practical reasons in this set-up, we prefer the Lagrange invariant to be limited by the path length ($Lp = 900\,\text{mm}$) between the second lens (L2) and the third lens (L3), as well as the diameter of the lenses L2 ($D_2 = 11.6\,\text{mm}$) and L3 ($D_3 = 26.6\,\text{mm}$). The expression for the Lagrange invariant (H) of the system can be written as†

$$H = \frac{D_2 D_3}{4Lp} = 0.086\,\text{mm}. \tag{3}$$

The instrument contribution to the phase difference between different parts of the object can be understood by the following consideration. When we remove the object and let a plane wave enter the instrument along the optical axis, these wave fronts will be parallel to the object and constitute a reference phase for different parts of the object plane. If the wave fronts do not remain planar after this wave is split into two parts and recombined by the beamsplitter BS2, they will produce undesirable fringes which could be mistaken as part of the phase structure of the object. To obtain a plane wave front at this point we design the optics collecting light from the object (L1, L2) as a beam-expanding telescope, which means the distance between L1 and L2 equals the sum of the focal lengths of each lens.

With appropriate stops to avoid vignetting, we let L1 (focal length 10 mm) image the object at L2 (focal length 90 mm), and L2 image L1 at L3 (focal length 400 mm). Finally L3 makes an image of L2, and thereby the object at the camera.

† For an object of size D_0 the Lagrange invariant may be written as $H = 0.5D_0$ (NA). In our design the NA of the system is about 0.13.

The final lens group L3 is chosen to make a sharp image of the object at the CCD camera†.

The quality of an imaging system can be characterized by the Strehl ratio (SR) of the system. Generally a system will be considered as diffraction-limited if the SR is greater than 0.8 [13]. The SR of our system, calculated by the optical design program ICON [14], is about 0.9 for an object of size $D_0 = 0.65\,\text{mm}$; in the centre of the object the best focus gives SR = 0.96. The change in the phase difference between lateral points in the object has been corrected to less than 0.1 wavelength for an object size of 0.65 mm.

The phase shift δ between the two sheared beams is introduced by using the wave-plate set (WP) shown in figure 1 to perform PSI. The basic concept is to orient the polarization directions of the two counter-propagating beams inside the triangular ring so one beam passes with its polarization parallel to the fast axis of the wave plate, and the other beam passes with polarization parallel to the slow axis, so these two beams will experience a relative optical phase delay. In this way four different steady-state phase shifts between the beams are introduced in turn, the interferograms for each are recorded, and pixel-by-pixel computations on the interferograms are performed afterwards in order to extract the SCF. The basic technique of phase shifting and pixel-by-pixel computation is utilized in modern commercial Twyman–Green and Fizeau interferometers for optical lens testing [10], and we have applied this technique to a Sagnac interferometer.

We developed the following procedure to apply the above principles to our optical system:

(1) Measuring the real part of SCF:
The wave-plate set consists of two half-wave plates. First we align the fast axes of both wave plates with the polarization direction of the input light, so the two counter-propagating beams experience a relative zero phase shift, and then record a series of interferograms, $I^{(0)}(x,s)$, with different amounts of shear s. See equation (2). Next we rotate the axes of one of the half-wave plates by 45°, which rotates the polarization of the beam by 90° when it passes through this wave plate. Note that one beam inside the triangular ring will have its polarization rotated before it passes through the second wave plate, while the other beam passes through the second wave plate first and then its polarization is rotated. Therefore the two counter-propagating beams experience a relative phase shift $\delta = \pi$ in passing through the other half-wave plate. Recording these interferograms yields $I^{(\pi)}(x,s)$. By subtracting $I^{(0)}(x,s)$ and $I^{(\pi)}(x,s)$ we remove the first two terms in the right-hand side of equation (2). Hence we obtain the real part of the SCF.

† Off-the-shelf achromatic doublets are designed to be optimal when the object is at infinity. When the object comes close to the lens, the aberrations increase, often by a large amount. In this set-up, we reduce aberrations by using two achromats to form a lens group for L3. The first achromat is turned around so that the ordinary image plane is located at the lens L2. Then the light from a point in the object is collimated after passing through the achromat, therefore working at its designed conjugate positions, and the aberrations are small. The other achromat is turned the 'right' way, with the ordinary image plane at the CCD camera, picking up the collimated light from the first achromat.

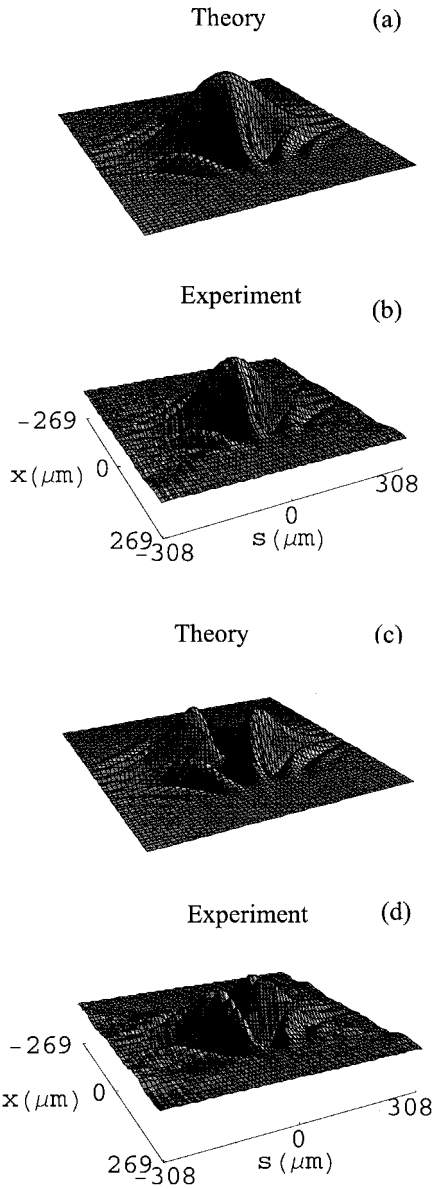

Figure 2. Measured SCF, versus position x and shear s. (a) and (c) show the prediction of the theory for the real and imaginary part respectively of the SCF. (b) and (d) show the results of measurements of the real and imaginary part respectively of the SCF.

(2) Measuring the imaginary part of SCF:
Adding a quarter-wave plate to the original wave plate set introduces an extra relative phase shift $\frac{1}{2}\pi$, and a factor $\exp[\mathrm{i}(\pi/2)] = \mathrm{i}$ in the last term in equation (2), making this term become the imaginary part of the SCF. Repeating a procedure similar to that above, we obtain the imaginary part of the SCF.

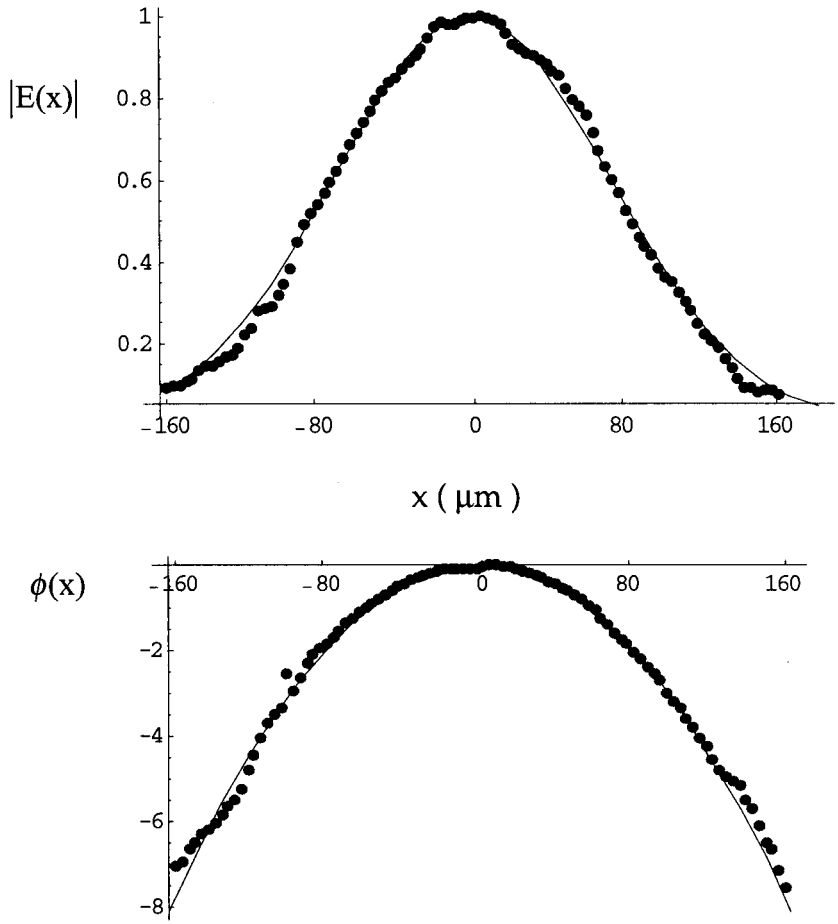

Figure 3. Reconstruction of amplitude $|E(x)|$ and phase $\phi(x)$ of the Gaussian beam from the data shown in figure 2. Circles are measured; solid curve is from theory.

This procedure correctly removes the first two terms in the right-hand side of equation (2) even if the two beamsplitters used in figure 1 have reflectivities that differ significantly from 50% for both polarizations of light, as long as these two reflectivities are equal. This can be understood by a careful analysis of the reflectivity and transmissivity the two beams experience when they are reflected by or transmitted through the beamsplitters†.

We performed a test measurement on a converging coherent Gaussian beam from a linearly polarized, continuous-wave He–Ne laser of wavelength 632.8 nm, having a $1/e$ half-width equal to 0.10 mm, and radius of wave-front curvature 15 mm in the (object) plane of measurement. Figure 2 shows comparisons between the resulting measurements of the SCF and the Gaussian-beam theoretical prediction for the same case. The frequency of oscillation in these functions depends on the radius of curvature of the wave fronts.

† By rotating the beamsplitters, we can partly equalize the reflectivities R_p and R_s for p- and s-polarized light. Our best results are $R_p = 0.51$ and $R_s = 0.53$.

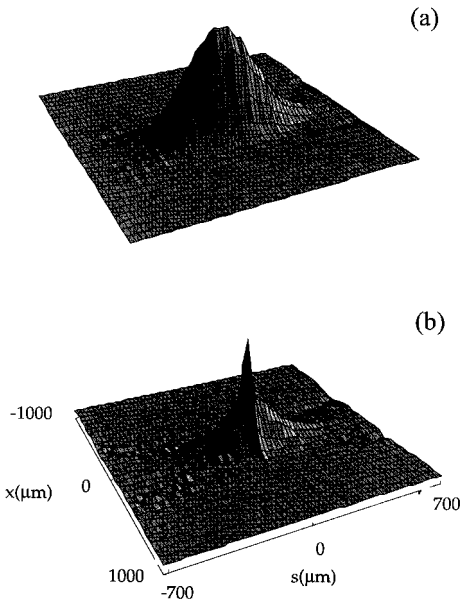

Figure 4. Evolution of SCF of the light from (*a*) coherent to (*b*) partially coherent, as light is scattered by a random medium. The volume fraction of the spheres in the medium used in (*b*) is 2%, corresponding to 1.36 average scattering events.

By inspecting equation (1) we can obtain the amplitude $|E(x)|$ and phase $\phi(x)$ of the light field, $E(x) = |E(x)| \exp[i\phi(x)]$, from the SCF values along the line $s = 2x$ by using

$$|E(2x)| = \frac{|\Gamma(2x,0)|}{[\Gamma(0,0)]^{1/2}} \tag{4}$$

and

$$\phi(2x) = \tan^{-1}\left(\frac{\mathrm{Im}\,[\Gamma(2x,0)]}{\mathrm{Re}\,[\Gamma(2x,0)]}\right) + \text{constant}. \tag{5}$$

The results, extracted from experimental and theoretical values in figure 2, are shown in figure 3. The agreement, obtained with no free parameters, is excellent, indicating that the system functions properly.

To demonstrate a measurement of a typical SCF of partially coherent light, we analysed a collimated Gaussian beam ($1/e$ half-width 0.14 mm) after it passed through a random, multiple-scattering medium (composed of polystyrene microspheres of diameter 46 μm suspended in a solidified gelatin–water mixture). The output face of the medium was located at the object plane (S), and was translated in the direction perpendicular to the beam axis while CCD images were acquired. This served to average the scattering over an ensemble of different sphere configurations, leading to partial destruction of the beam s transverse coherence [8]. For a collimated Gaussian beam the real part of the SCF contains no oscillations since the radius of wave-front curvature was infinite, which leads to the imaginary part being zero. Figure 4 shows the evolution of the real part of the measured SCFs from coherent input field (figure 4 (*a*)) to partially coherent transmitted field (figure 4 (*b*)). In figure 4 (*b*) the rapid decay of the SCF seen in the s-direction clearly indicates the loss

of transverse coherence. We have obtained a quantitative agreement between this measured SCF and a theory of light scattering, providing further evidence that our system yields accurate measurements of the SCF of partially coherent light [8].

4. Conclusion

Our system has improved on light collection and reduced aberrations so that it can be used reliably in measuring strongly divergent light, for example, the quasi-straightforward propagating (QSP) light discussed in the context of bio-tissue imaging [15]. This simple, robust design operates without the requirement of a carefully stabilized environment because common-path interferometry is employed.

From the measurement of the SCF we can calculate various statistical moments of the field distribution for beam quality characterization. For instance we can evaluate the beam quality factor M^2 for coherent laser beams [16]. It might be possible to generalize the concept of M^2 to include the case of partially coherent light, which can be analysed by our system. Also by a proper Fourier transform of the SCF we can calculate the Wigner function of the light field, which is an important quantity in wave transport [8], classical optics, as well as quantum optics [17].

Acknowledgments

This work is supported in part by the Army Research Office and by DOE through the Oregon Medical Laser Center. MR thanks NDRE for hospitality during his extended stay there, where a portion of this work was done.

References

[1] Mandel, L., and Wolf, E., 1995, *Optical Coherence and Quantum Optics* (New York: Cambridge University Press), Chap. 4.
[2] John, S., Pang, G., and Yang, Y., 1996, *J. Biomed. Optics*, **1,** 180.
[3] Komberg, B. V., Kravtsov, A. V., and Lukash, V. N., 1994, *Astron. Astrophys.*, **286,** L19.
[4] Kravtsov, Yu. A., and Apresyan, L. A., 1996, *Progress in Optics*, Vol. XXXVI, edited by E. Wolf (Amsterdam: North-Holland), p. 179.
[5] Zarubin, A. M., 1996, *Ultramicroscopy*, **62,** 229; 1991, *Optics Commun.*, **100,** 491.
[6] Francon, M., and Mallick, S., 1967, *Progress in Optics*, Vol. VI, edited by E. Wolf (Amsterdam: North-Holland), pp. 73–104.
[7] Iaconis, C., and Walmsley, I. A., 1996, *Optics Lett.*, **21,** 1783.
[8] Chung-Chieh Cheng and Raymer, M. G., 1999, *Phys. Rev. Lett.*, **82,** 4807.
[9] Wax, A., and Thomas, J. E., 1998, *J. opt. Soc. Am.* A, **15,** 1896.
[10] Greivenkamp, J. E., and Bruning, J. H., 1992, *Optical Shop Testing*, edited by D. Malacara (New York: John Wiley & Sons), Chap. 14.
[11] McAlister, D., Beck, M., Clarke, L., Mayer, A., and Raymer, M. G., 1995, *Optics Lett.*, **20,** 1181.
[12] Mantravadi, M. V., 1992, *Optical Shop Testing*, edited by D. Malacara (New York: John Wiley & Sons), Chap. 4.

[13] See for example Palmer, J. R., 1993, *Proc. SPIE*, **1869,** 36.
[14] ICON lens design program, GEMINALI ANS, Oslo, Norway.
[15] Horinaka, H., Hashimoto, K., Wada, K., and Cho, Y., 1995, *Opt. Lett.*, **20,** 1501.
[16] Siegman, A. E., 1990, *Proc. SPIE*, **1224,** 2; Bélanger, P.-A., Champagne, Y., and Paré, C., 1994, *Optics Commun.*, **105,** 233.
[17] Raymer, M. G., Beck, M., and McAlister, D. F., 1994, *Phys. Rev. Lett.*, **72,** 1137.